Supporting Information

Lewis basic CeO_2 cocatalyst expedites two-electron air electroreduction at theoretical limit

Lili Jiang,[a] Shan Ding,[a] Haiyun Li,[a] Jingjing Duan,[a] Minmin Yan,*[a] Sheng Chen*[a]

DOI:

Supplementary Information

Table of Contents

1. Experimental Procedures....3

  1.1 Materials synthesis....3

  1.2 Physical characterizations....3

  1.3 Electrochemical Characterization....3

  1.4 DFT calculation details....5

2. Supplementary Results....7

3. References....21

1. Experimental Procedures

1.1 Materials synthesis

1) Synthesis of ZnO

1.10 g of $Zn(CH_3COO)_2\cdot 2H_2O$ was dissolved in 100 mL of ethanol and refluxed at 78 °C for 2 h. After the solution cooling to room temperature, 2.5 mL of $(CH_3)_4NOH$ was added in the solution and performed hydrolysis in an ultrasonic bath for 30 min to obtain a ZnO precursor solution. Next, 1.0 mL of the prepared ZnO precursor solution was added into a mixture of 30 mL containing 10 mM $Zn(NO_3)_2\cdot 6H_2O$ and 10 mM hexamethylenetetramine (HMT). Then, the mixture was stirred thoroughly and transferred into a reaction vessel to react at 90 °C for 3 h. Following the reaction, the mixture was centrifuged and washed for three times. After freeze-drying, ZnO samples were obtained. To prepare a series of 1D ZnO samples with varying dimensions, adjust the concentrations of $Zn(NO_3)_2\cdot 6H_2O$ and HMT to 1 mM, 3 mM, 5 mM and 10 mM, respectively.

The chemical deposition process using $Zn(NO_3)_2\cdot 6H_2O$ and HMT as reactants can be represented by the following equation:

$$(CH_2)_6N_4 + 6H_2O \rightarrow 6HCHO + 4NH_3 \qquad (1)$$

$$NH_3 + H_2O \leftrightarrow NH_4^+ + OH^- \qquad (2)$$

$$2\ OH^- + Zn^{2+} \rightarrow Zn\ (OH)_2 \leftrightarrow ZnO + H_2O \qquad (3)$$

2) Synthesis of ZnO/CeO_2

The CeO_2 layer was coated on the surface of 1D ZnO by the thermal decomposition coating method. $Ce(NO_3)_3\cdot 6H_2O$ was dissolved in ethanol to prepare solutions of 0.025 M, 0.05 M, 0.075 M, 0.10 M and 0.15 M. Then, 30 mg of ZnO powder was added to each of the above solutions of different concentrations and stirred for 1 h. After centrifugation and drying, the samples were calcined in an Ar atmosphere at 400 °C for 3 h with a heating rate of 2 °C min^{-1}, resulting in a series of ZnO/CeO_2 samples, which were labeled as ZnO/CeO_2-0.025 M, ZnO/CeO_2-0.05 M, ZnO/CeO_2-0.075 M, ZnO/CeO_2-0.1 M and ZnO/CeO_2-0.15 M respectively.

1.2 Physical characterizations

The morphology, lattice fringes and electron diffraction patterns of the samples were characterized by high-resolution transmission electron microscopy (HRTEM, FEI Tian 80-300, 300 kV accelerating voltage). The crystal structure of the samples was characterized by X-ray diffraction (XRD, Smartlab, 9 kW, 40 kV, 40 mA, $\lambda = 1.5418$ Å). the valence state and electronic environment of the elements in the samples were characterized by X-ray photoelectron spectroscopy (XPS, Axis Ultra, Thermo ESCALB 250XI, Radiation with an Al Kα source, 1486.6 eV, Collect signals within the range of 0 to 1400 eV).

1.3 Electrochemical Characterization

1) Electrochemical test on rotating ring disk electrode (RRDE)

The intrinsic activity of the samples for ORR was evaluated using a rotating ring disk electrode (RRDE) setup from PINE Instruments, USA. The RRDE with an electrode area of 0.2475 cm^2 was used as the working electrode, a graphite rod electrode as the counter electrode, and an Ag/AgCl electrode as the reference electrode to form a three-electrode test system for the measurements in the 0.6 M K_2SO_4 electrolyte. The ring collection efficiency (*N*) of RRDE was determined to be 0.365 using a typical redox couple of potassium ferricyanide solution. The working electrode was prepared by the solution casting method. Specifically, 5 mg of catalyst, 0.5 mg of acetylene black, and 30 μL of Nafion (5 wt%) were dissolved in 970 μL of isopropanol/deionized water (3:1, v/v), and the mixture was sonicated for 1 h to form a uniform catalyst slurry. Then, 10 μL of the slurry was dropped onto the disk electrode to form a uniform catalyst layer, which was dried overnight in a natural environment. The activity and selectivity of the samples were investigated by linear sweep voltammetry (LSV) measurement at 1600 rpm in O_2-saturated electrolyte, and the Pt ring electrode potential was maintained at 1.2 V (vs. RHE) to quantify the amounts of H_2O_2 produced on the disk electrode.

The H_2O_2 selectivity and number of transferred electrons (*n*) were calculated respectively by the following formulas through the disk current and the oxidation current of H_2O_2 on the platinum ring:

$$\mathrm{H_2O_2\ selectivity\ (\%)} = \frac{200 \times \frac{I_r}{N}}{|I_d| + \frac{I_r}{N}} \tag{4}$$

$$n = \frac{4 \times |I_d|}{|I_d| + \frac{I_r}{\mathrm{N}}} \tag{5}$$

I_d represents the disk current, I_r represents the ring current, and *N* is the RRDE current collection efficiency. All the test potentials in the paper are referenced to the reversible hydrogen electrode potential, according to the following formula:

$$E_{\mathrm{RHE}} = E_{\mathrm{Ag/AgCl}} + 0.059\ \mathrm{pH} + 0.197 \tag{6}$$

2) Electrochemical test on a flow cell

The potential of oxygen reduction to produce H_2O_2 at industrial current densities was evaluated using a flow electrolytic cell. The working electrode was prepared by the solution casting method. Specifically, 5 mg of sample, 0.5 mg of acetylene black, and 30 μL of Nafion solution (5 wt%) were dispersed in 970 μL of isopropanol/pure water (3:1, v/v), and then sonicated for about 1 h to form a uniform catalyst slurry. 1 mL of uniform catalyst slurry was sprayed evenly onto a 1×1 cm^2 gas diffusion electrode. The electrocatalytic oxygen reduction performance was tested on a CHI 760E electrochemical workstation connected with a CHI 680C current amplifier. The standard three-electrode three-phase flow cell was assembled with the following components: the gas diffusion electrode sprayed with the catalyst was used as the working electrode, a coated titanium anode (Dimensionally Stable Anode, DSA, 2×2 cm^2) was used as the counter electrode, and an Ag/AgCl electrode (saturated KCl solution) was used as the reference electrode. The Nafion 117 membrane was used as the proton exchange membrane to separate the anode chamber from the cathode chamber. The electrolyte was 0.6 M K_2SO_4, which was circulated in the flow cell at a flow rate of 40 rpm min^{-1} by a peristaltic pump.

All electrochemical data were not corrected for iR, and the current density was normalized to the geometric area. The hydrogen peroxide yield (H_2O_2, mg h^{-1} cm^{-2}) and Faraday efficiency (FE, %) were calculated by the following formula:

$$Y\,(H_2O_2) = c\,(H_2O_2) \times V\,/\,(t \times S) \tag{7}$$

$$FE_{H2O2}\,(\%) = 2F \times c\,(H_2O_2) \times V\,/\,(34 \times Q) \tag{8}$$

c (H_2O_2) represents the concentration of H_2O_2, V is the volume of the electrolyte solution, t is the reaction time, S is the electrode area, F is the Faraday constant, and Q is the total charge passed.

3) Determination of H_2O_2 concentration by traditional titration method with $Ti(SO_4)_2$

The traditional titration method was adopted to determine the concentration of H_2O_2. This method is based on the reaction between colorless $Ti(SO_4)_2$ solution and H_2O_2 to form a yellow H_2TiO_4 complex ($Ti^{4+} + H_2O_2 + 2H_2O \rightarrow H_2TiO_4 + 4H^+$). This yellow complex can be measured by ultraviolet-visible spectrophotometry, which has an ultraviolet absorption peak at a wavelength of 408 nm. According to Lambert-Beer's law, the concentration is directly proportional to the absorbance, and the corresponding H_2O_2 concentration can be calculated. The details of method were described as bellow: First, prepare a 0.6 M K_2SO_4 electrolyte solution. Then, use a 30 wt% commercial H_2O_2 solution to prepare a series of H_2O_2 solutions with known concentrations ranging from 0 to 140 ppm. Next, take 9 mL of the above solutions with known concentrations, add 1 mL of titanium sulfate color reagent, mix well, and conduct ultraviolet testing to obtain a series of UV-Vis curves at different concentrations. Take the absorbance at a wavelength of 408 nm and perform linear fitting based on the concentration and absorbance to draw the quantitative standard curve of H_2O_2. As shown in Figure S3, the correlation coefficient R2 of this curve reaches 0.9999, which can be used as the basis for subsequent quantitative determination of H_2O_2.

1.4 DFT calculation details

DFT calculations were performed by the MedeA-VASP Package. The convergence criteria for electronic self-consistent iterations (SCF) and energy were set at 0.05 eV/Å and 10^{-5} eV. The exchange-correlation potential was defined through using The Perdew-Burke-Ernzerhof (PBE) generalized gradient approach[1]. The plane wave energy cutoff of structure optimization was set to be 400 eV and precision was set at normal. We use the projector augmented wave method (PAW) to describing the interaction between the atomic cores and electrons[2]. Gaussian smearing with a width of 0.05 to 0.2 eV. In the real space, the integration of the surface Brillouin zone was used with a 1×1×1 MonkhorstPack K-point grid. The Hubbard-U correction method (DFT+U) was utilized to improve the description of highly correlated Zn 3d orbitals and Ce 4f orbitals, with the value of U-J set to be 2.5 eV and 5.0 eV, respectively.

The detailed 2e⁻ ORR Gibbs free energy has been calculated according to the following equation in:

$$G = E + ZTE - TS$$

In this formula, G, E and ZTE correspond to chemical Gibbs free energy, electronic energy and zero-point energy, respectively. The entropy can be calculated through the sum of the vibrational, rotational, translational, and electronic can be made a contribution to:

$$S = S_v + S_r + S_t + S_e$$

Since $S_e \approx 0$ at the fundamental electronic level.

For the condition of solids and adsorbates, some approximations can be adopted: Translational and rotational motions can be missed, hence, $S_t \approx 0$ and $S_r \approx 0$. In this circumstance, all the entropy values come from the vibrational contribution: $S = S_v$

Therefore, Gibbs free energy for distinct states can be calculated as to:

$$G = E + ZTE - TS_v$$

For the details on the computational model of ZnO/CeO_2: the lattice mismatch between ZnO and CeO_2 is less than 5%, with their lattice parameters *a* and *b* differing by 3.31% and 0.90%, respectively. Figure S9 displays the interfacial region of ZnO/ CeO_2 and compares the residual stress distribution at the interface before and after geometry optimization. The oxygen vacancy concentration in the ZnO/ CeO_2 model is approximately 7%.

2. Supplementary Results

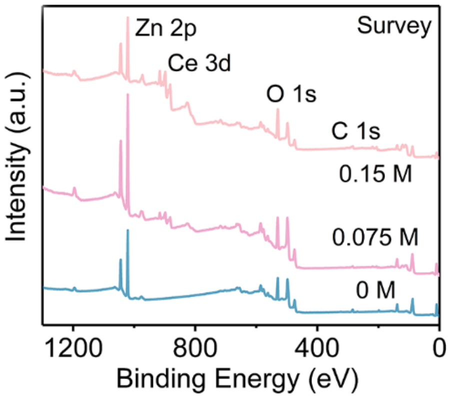

Figure S1 XPS survey spectrum of ZnO/CeO_2 synthesized with different concentrations of $Ce(NO_3)_3$.

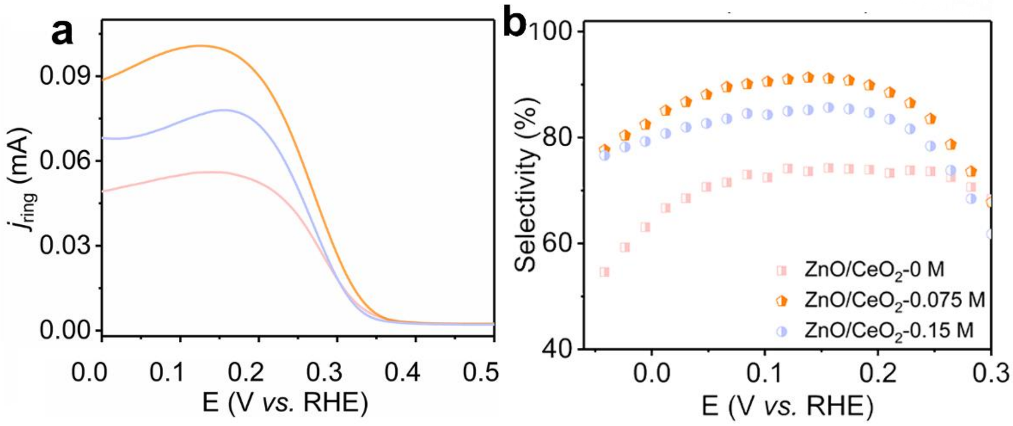

Figure S2 Oxygen reduction performance test of ZnO/CeO$_2$ on RRDE. (a) Ring current obtained by LSV test at a rotation speed of 1600 rpm, a scan rate of 5 mV s^{-1}, and a fixed potential of 1.2 V (vs. RHE). (b) Selectivity calculated from LSV test.

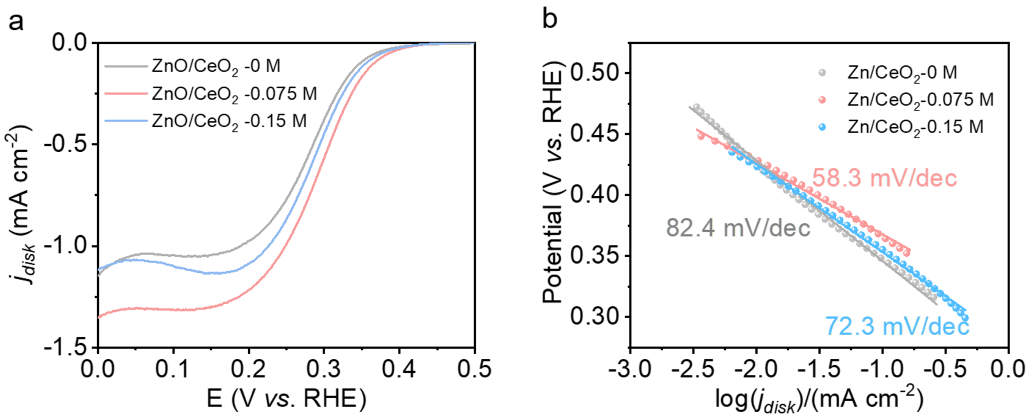

Figure S3 (a) The LSV curves and (b) Tafel slop of ZnO/CeO$_2$-0M, ZnO/CeO$_2$-0.075M and ZnO/CeO$_2$-0.15M tested by RRDE in O_2 feed 0.6 M K_2SO_4 solution.

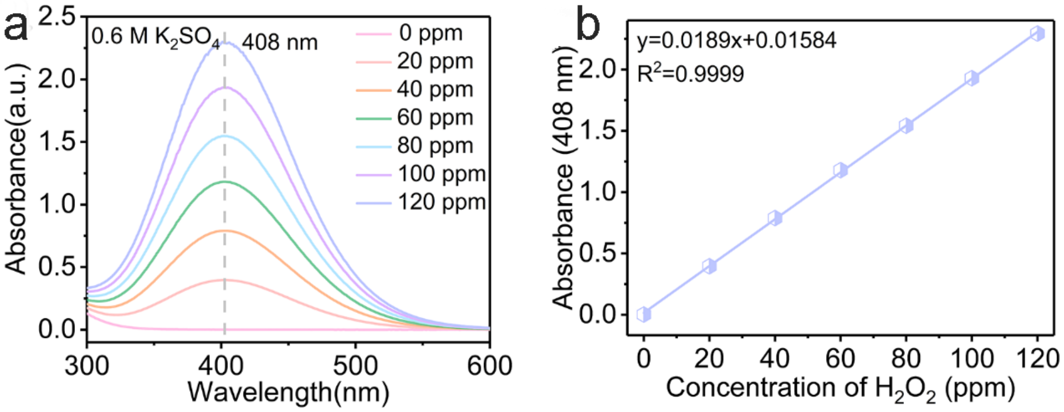

Figure S4 The standard curve for H_2O_2 was determined by the traditional titration method with titanium sulfate in 0.6 M K_2SO_4 electrolyte. (a) The UV-Vis curves of H_2TiO_4 generated from different concentrations of H_2O_2 at the range of 300 – 600 nm. (b) Linear calibration curve based on the peak absorbance at 408 nm.

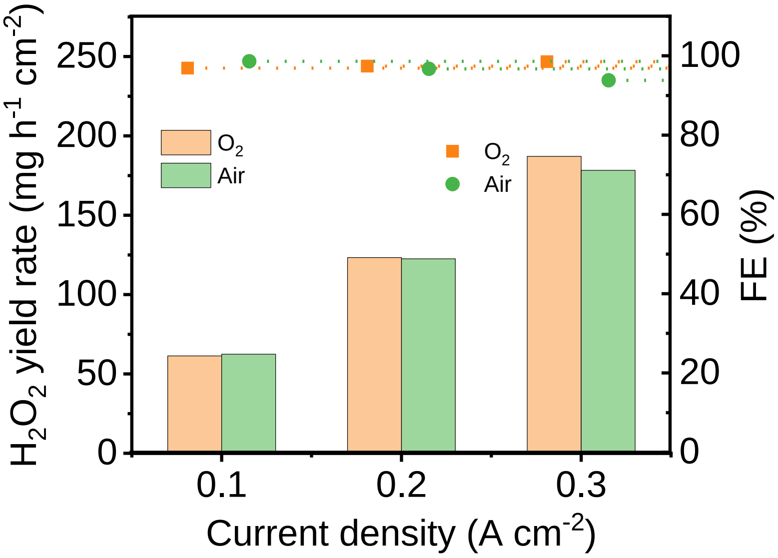

Figure S5. H_2O_2 yield rate and Faradaic efficiency (FE) of ZnO/CeO_2-0.075 M in different current density by O_2/Air feed.

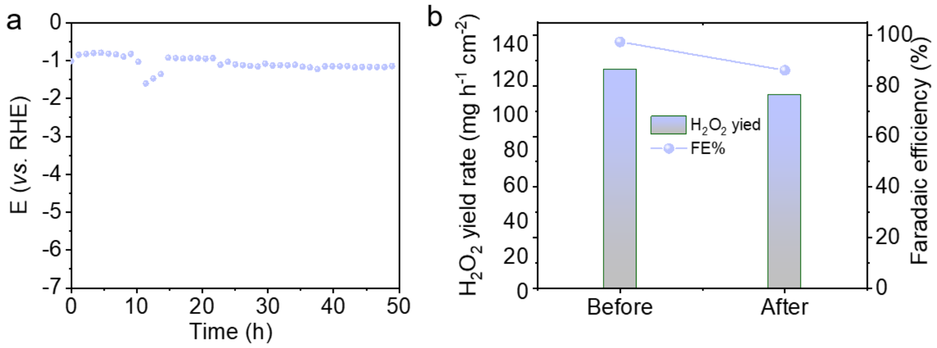

Figure S6 (a) Chronopotentiometric stability test of ZnO/CeO_2-0.075M for 50 hours under air feed at a current density of 0.2 A cm^{-2}. (b) The comparison of H_2O_2 yield rate and Faradaic efficiency before and after stability test.

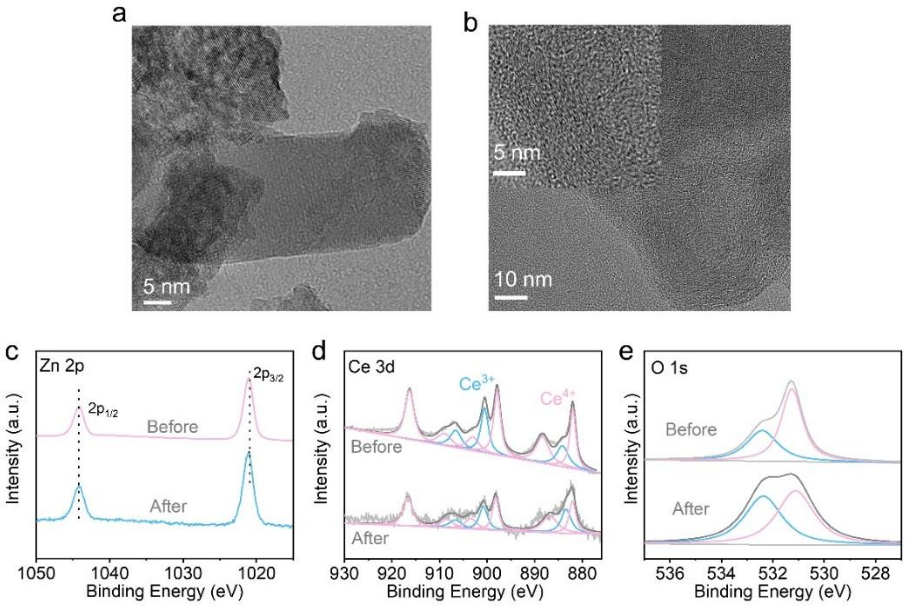

Figure S7 TEM images of ZnO/CeO$_2$ before (a) and after (b) stability test. High-resolution Zn 2p (c), Ce 3d (d) and O 1s (e) XPS spectra of ZnO/CeO$_2$ before and after stability test.

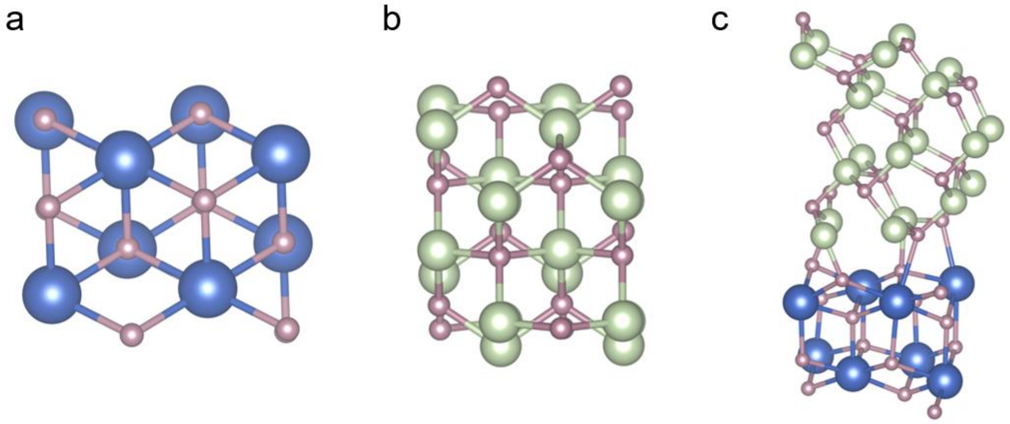

Figure S8 (a) The (111) facet of CeO_2, (b) the (101) facet of ZnO and (c) the theoretical model of ZnO/CeO_2.with oxygen vacancies (~4% *vs.* ~7% *vs.* ~7%).

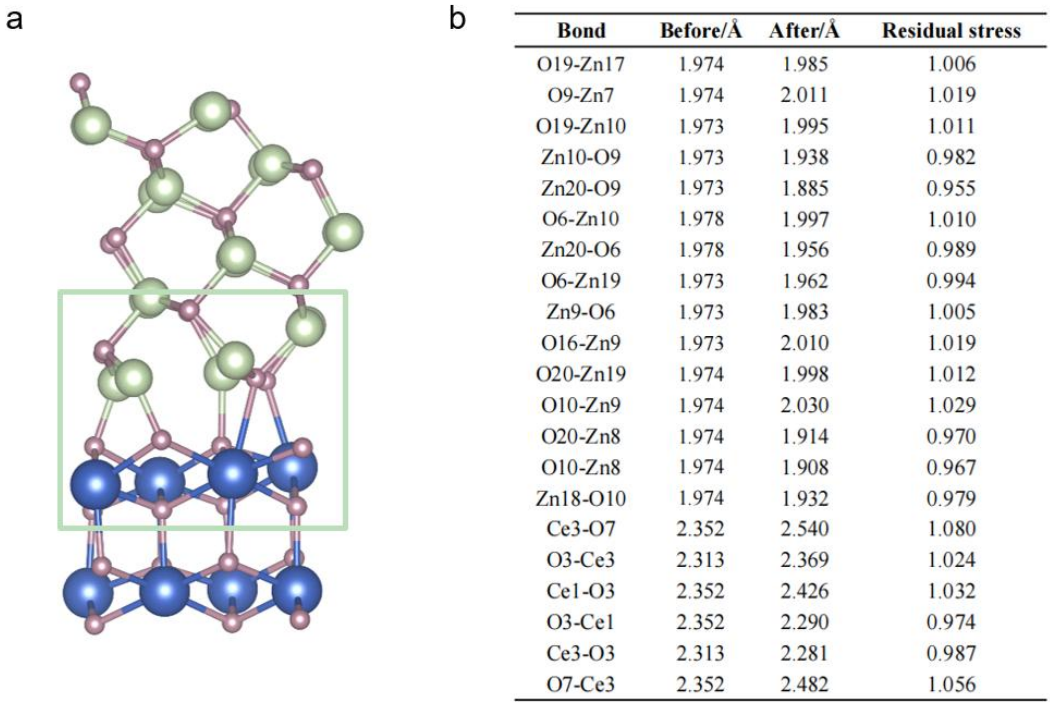

Bond	Before/Å	After/Å	Residual stress
O19-Zn17	1.974	1.985	1.006
O9-Zn7	1.974	2.011	1.019
O19-Zn10	1.973	1.995	1.011
Zn10-O9	1.973	1.938	0.982
Zn20-O9	1.973	1.885	0.955
O6-Zn10	1.978	1.997	1.010
Zn20-O6	1.978	1.956	0.989
O6-Zn19	1.973	1.962	0.994
Zn9-O6	1.973	1.983	1.005
O16-Zn9	1.973	2.010	1.019
O20-Zn19	1.974	1.998	1.012
O10-Zn9	1.974	2.030	1.029
O20-Zn8	1.974	1.914	0.970
O10-Zn8	1.974	1.908	0.967
Zn18-O10	1.974	1.932	0.979
Ce3-O7	2.352	2.540	1.080
O3-Ce3	2.313	2.369	1.024
Ce1-O3	2.352	2.426	1.032
O3-Ce1	2.352	2.290	0.974
Ce3-O3	2.313	2.281	0.987
O7-Ce3	2.352	2.482	1.056

Figure S9 (a) The range of the interface in ZnO/CeO_2 and (b) the residual stress of the bond between interface of ZnO/CeO_2 before and after geometry optimization.

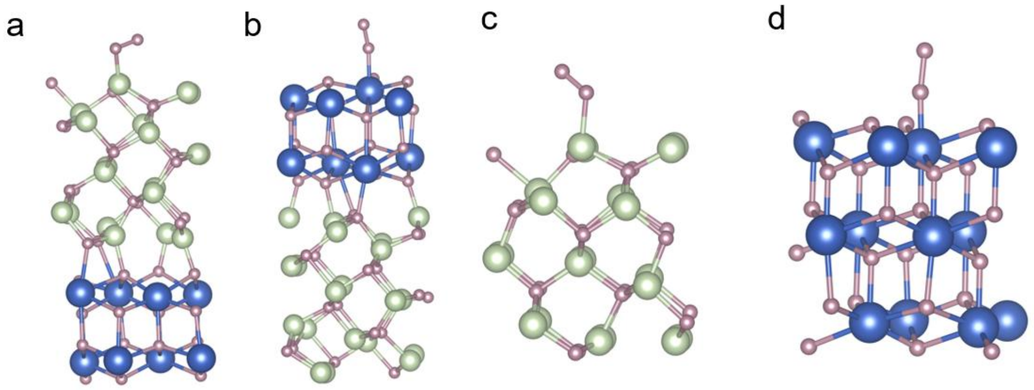

Figure S10 The theoretical model of absorption O_2 on the Zn (a) and Ce (b) sites in ZnO/CeO_2, the Zn (c) sites in ZnO and Ce (d) sites in CeO_2.

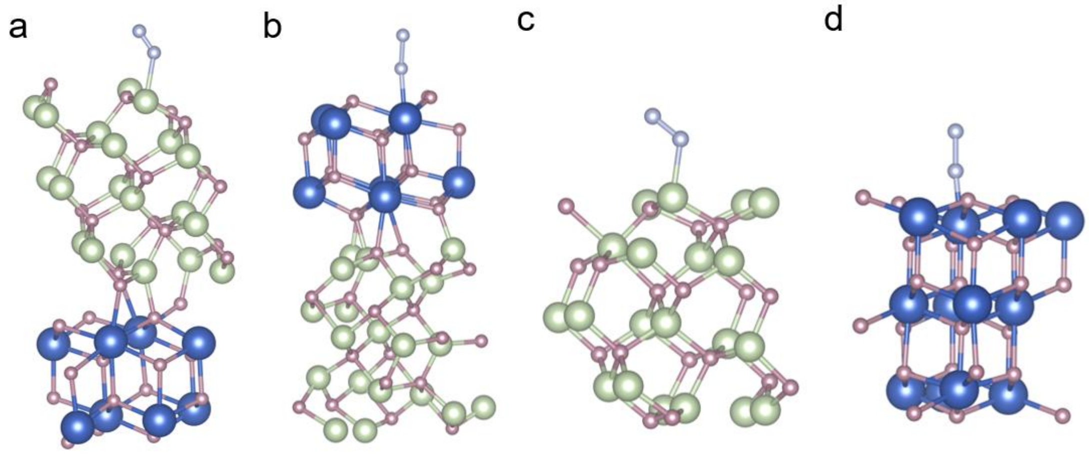

Figure S11 The theoretical model of absorption N_2 on the Zn (a) and Ce (b) sites in ZnO/CeO_2, the Zn (c) sites in ZnO and Ce (d) sites in CeO_2.

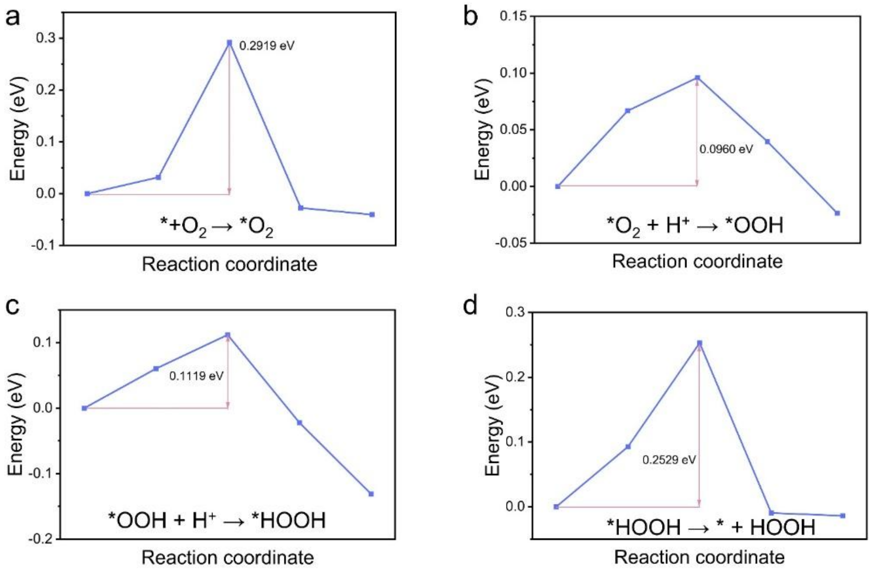

Figure S12 Minimum energy path (MEP) of ZnO/CeO_2 ORR pathway, including (a) * + O_2 → *O_2, (b) *O_2 + H^+ → *OOH, (c) *OOH + H^+ → *HOOH and (d) *HOOH → * + HOOH. Initial, transition and final states were included of the image.

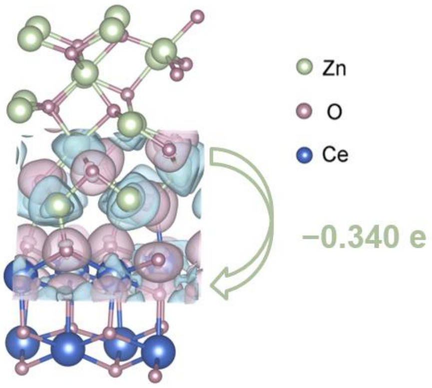

Figure S13 The difference charge density of ZnO/CeO_2.

Table S1 The calculation details of the adsorption energy of O_2 and N_2 on Zn sites of ZnO/CeO_2 and ZnO, Ce sites of ZnO/CeO_2 and CeO_2.

	E_{ads}/eV	$E_{Surface}$/eV	$E_{molecular}$/eV	Adsorption energy/eV
O_2-ZnO/CeO_2	-357.350981	-346.804789	-9.91	-0.636192
N_2-ZnO/CeO_2	-363.643699	-346.804789	-17.016409	0.177499
O_2-CeO_2/ZnO	-356.493591	-346.491432	-9.91	-0.092159
N_2-CeO_2/ZnO	-358.324615	-346.491432	-17.016409	5.183226
O_2-CeO_2	-292.540562	-284.609729	-9.91	1.979167
N_2-CeO_2	-301.424413	-284.609729	-17.016409	0.201725
O_2-ZnO	-168.059262	-158.679306	-9.91	0.530044
N_2-ZnO	-175.428227	-158.679306	-17.016409	0.267488

The specific calculation data of adsorption energy, Adsorption energy = $E_{ads} - E_{Surface} - E_{molecular}$.

3. References

[1] B. Perdew, Ernzerhof, *Phys. Rev. Lett.* 1996, **77**, 3865-3868.

[2] G. Kresse, Joubert, D., *Phys. Rev., B Condens. Matter* 1999, **59**, 1758-1775.